

## Supplementary Information (SI)

### Synergistic optimization of thermoelectric performance in $\text{Ag}_2\text{Se}$ through $\text{MoSe}_2$ decoration

Wajid Hussain<sup>1</sup>, Lei Yang<sup>2</sup>, Ziyang Zhou<sup>1</sup>, Peijie Ma<sup>1</sup>, Hu Hanwen<sup>1,3\*</sup>, Kun Zheng<sup>1,\*</sup>

**Table1**-Precursors used in the synthesis of  $\text{Ag}_2\text{Se}/\text{MoSe}_2$  composite samples with differing  $\text{MoSe}_2$  concentrations.

Sample name	$\text{NaBH}_4$ (g)	Se (g)	$\text{Na}_2\text{MoO}_4 \cdot 2\text{H}_2\text{O}$ (g)	$\text{Ag}_2\text{Se}$ (g)
AS-1	0.0078	0.0108	0.0164	2
AS-2	0.0156	0.0216	0.0328	2
AS-3	0.0234	0.0324	0.0492	2
AS-4	0.0312	0.0432	0.0656	2
AS-5	0.039	0.0540	0.0820	2

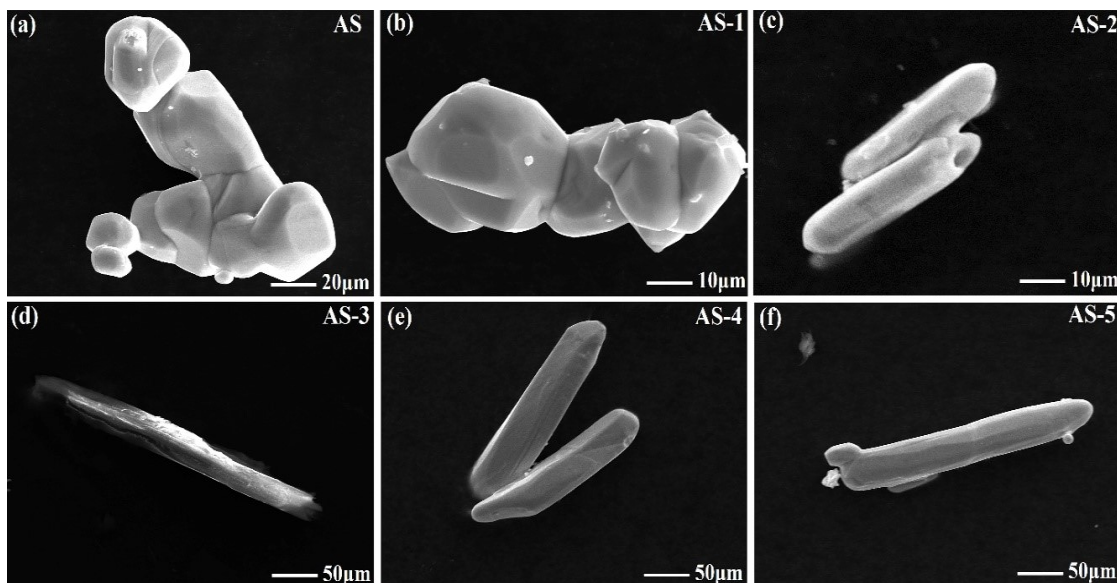


**Fig.S1.** Scanning Electron Microscopy (SEM) images of pure  $\text{Ag}_2\text{Se}$  and  $\text{Ag}_2\text{Se}/\text{MoSe}_2$  composites: (a) AS pure  $\text{Ag}_2\text{Se}$ , (b-f) AS-1 to AS-5  $\text{Ag}_2\text{Se}/\text{MoSe}_2$  with increasing amount of  $\text{MoSe}_2$  as (b) 1 mol% (c) 2 mol% (d) 3 mol% (e) 4 mol% (f) 5 mol%.

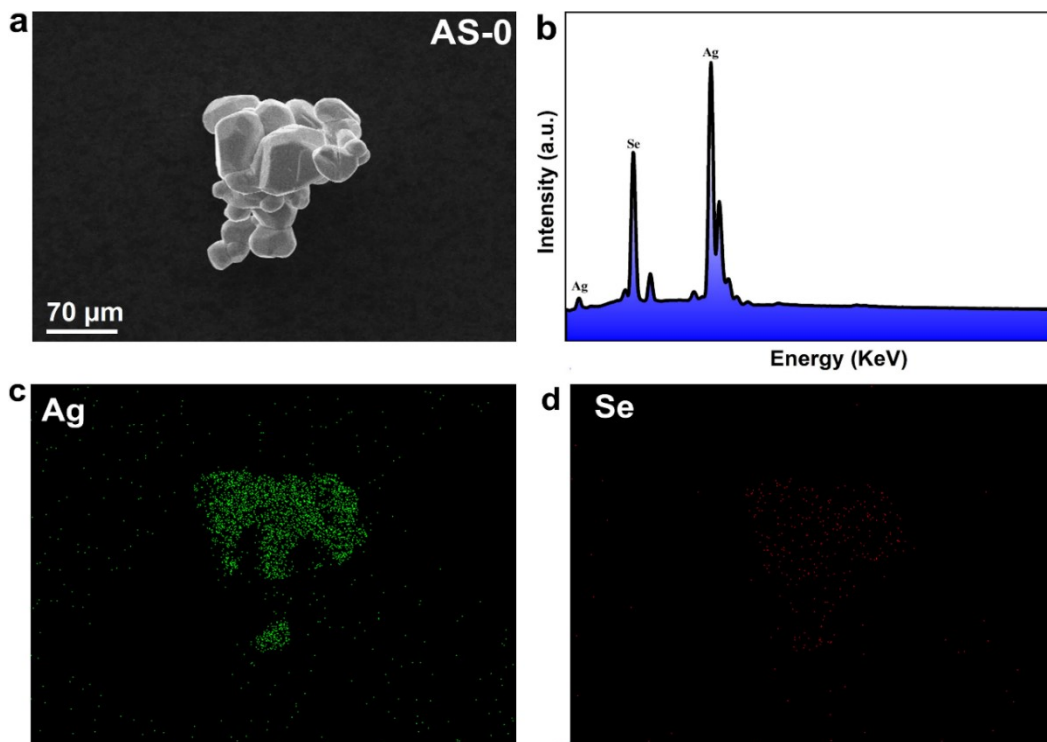


**Fig. S2:** (a) SEM image of AS-0 with a 70 μm scale bar. (b) EDS spectrum showing Ag and Se peaks. (c) Ag and (d) Se EDS mapping of the sample.

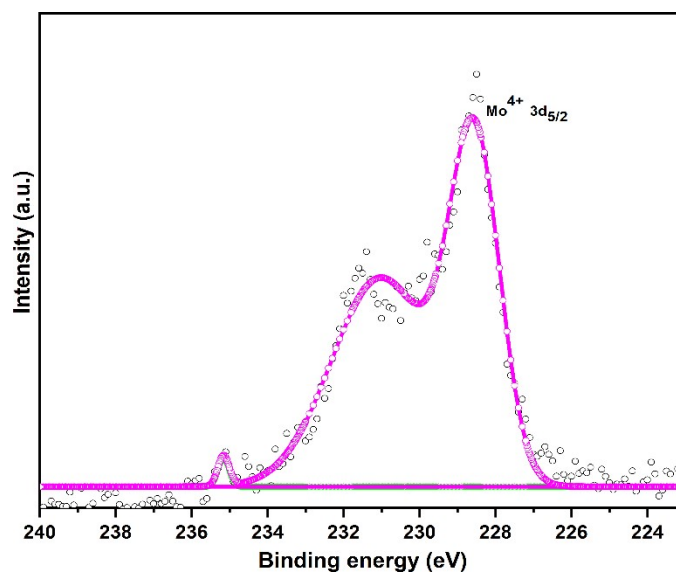


**Fig.S3.** Mo oxidation state on the powder surface is identified from Mo 3d XPS spectra, with weak shoulder peak at higher binding energies indicating Mo<sup>5+</sup>/Mo<sup>6+</sup> ions.

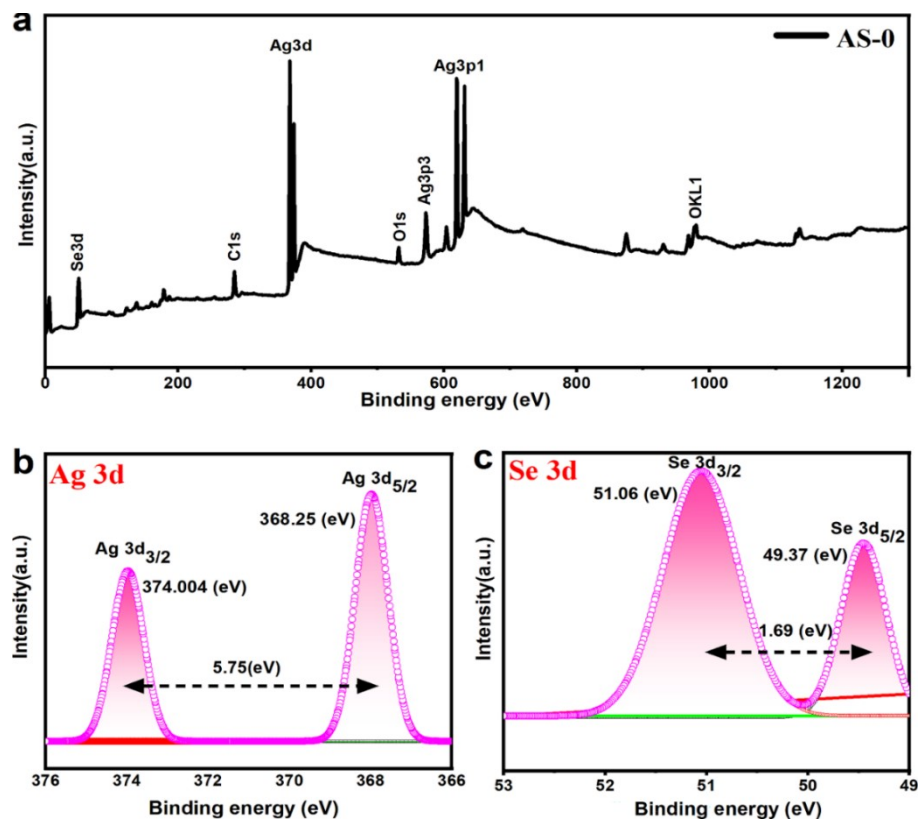


**Fig. S4.** XPS spectra of the AS-0 sample showing the survey scan (a) and high-resolution Ag 3d (b) and Se 3d (c) peaks, with corresponding binding energies and peak separations.

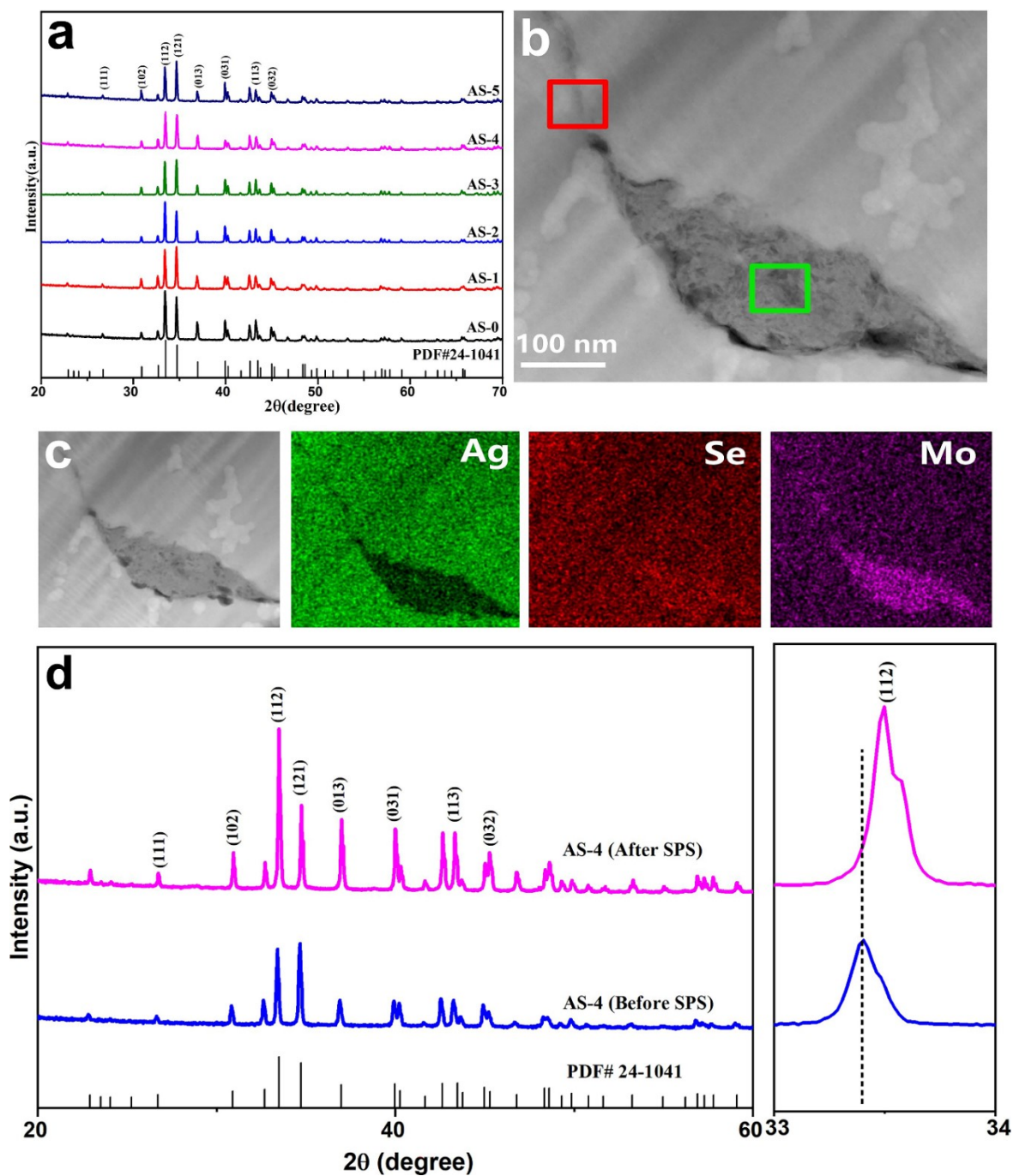


**Fig. S5.** (a) X-ray diffraction (XRD) patterns of composites; (b) high-resolution transmission electron microscopy (HRTEM) images, accompanied by (c) corresponding elemental maps of Ag, Se, and Mo, illustrating the uniform integration of  $\text{MoSe}_2$  inside the  $\text{Ag}_2\text{Se}$  matrix; (d) XRD pattern of AS-4 before and after SPS.

## Measurement of Thermoelectric Performance

### Hall Coefficient ( $R_h$ )

The Hall coefficient measures the charge carrier concentration in the material and is calculated using

$$R_h = \frac{v_H}{I \cdot B \cdot d}$$

( $V_H$ ) is the measured Hall voltage, ( $I$ ) is the current flowing through the material. ( $B$ ) is the magnetic field applied perpendicular to the current and ( $d$ ) is the thickness of the material through which the current flows.

### Hall Mobility ( $\mu_h$ )

Hall mobility gives the ease with which carriers can move in the presence of an electric field

$$\mu_h = \frac{R_h}{\rho}$$

Where ( $R_h$ ) is the Hall coefficient ( $\rho$ ) represent the resistivity of the material (inverse of conductivity).

### Electrical Conductivity ( $\sigma$ )

$$\sigma = \frac{1}{\rho}$$

Where  $\rho$  is resistivity

$$\sigma = \frac{L}{R \cdot A}$$

Where  $L$  is the length of the sample  $R$  is the measured resistance and  $A$  is the cross-sectional area of the material.

## Thermal Conductivity ( $\kappa$ )

Thermal conductivity can be calculated as

$$\kappa = \frac{Q.L}{A.\Delta T.t}$$

Where  $Q$  is the heat flow (in watts),  $L$  is the length through which heat flows,  $A$  is the cross-sectional area,  $\Delta T$  is the temperature difference and  $t$  show the time over which the heat transfer occurs.

## Seebeck Coefficient ( $S$ )

$$S = \frac{V}{A.\Delta T}$$

Where  $V$  is the voltage measured across the material and  $\Delta T$  is the temperature difference applied across the material

The Seebeck coefficient can be positive (for p-type materials) or negative (for n-type materials), indicating the type of carriers responsible for conduction.

## Power Factor (PF)

$$PF = S^2 \sigma$$

Where  $S$  is the Seebeck coefficient and  $\sigma$  is the electrical conductivity.

## Figure of Merit ( $zT$ )

The thermoelectric figure of merit ( $zT$ ) integrates electrical characteristics and thermal conductivity into a single dimensionless value, signifying a material's efficiency for thermoelectric applications.

$$zT = \frac{S^2 \cdot \sigma}{\kappa} T$$

S is the Seebeck coefficient,  $\sigma$  is the electrical conductivity, T is the absolute temperature (in Kelvin) and  $\kappa$  is the thermal conductivity.

### Wiedemann-Franz Law

The Wiedemann-Franz Law can be derived by examining the connection between thermal conductivity ( $\kappa$ ) and electrical conductivity ( $\sigma$ ) in metals, both of which are predominantly governed by the movement of free electrons. The electrical conductivity in metals is expressed by the following equation:

$$\sigma = \frac{ne^2\tau}{m} \quad (1)$$

where n is the electron density, e is the electron charge,  $\tau$  is the mean free time between collisions, and m is the mass of the electron. Thermal conductivity due to free electrons is expressed as

$$\kappa = \frac{1}{3}nCv^2\tau \quad (2)$$

where C is the specific heat capacity of electrons, v is their average velocity, and n and  $\tau$  are the same as in the conductivity equation. Since the electron specific heat C and velocity v are both temperature-dependent ( $C \sim T$  and  $v \sim \sqrt{T}$ )

$$\kappa \sim nT\tau \quad (3)$$

To relate the two conductivities, we divide the expression for  $\kappa$  by  $\sigma$ , leading to the equation:

$$\frac{\kappa}{\sigma} = \frac{(nT\tau)}{(ne^2\tau/m)} = \frac{mT}{e^2} \quad (4)$$

The constant  $\frac{m}{e^2}$  is recognized as the Lorenz number (L), giving the final form of the Wiedemann-Franz Law

$$\frac{\kappa}{\sigma} = L.T \quad (5)$$

$$L = 1.5 + \exp\left[-\frac{|S|}{116}\right]$$

### Phonon Scattering Mechanisms and the Callaway Model for Thermal Conductivity

The Callaway model is a detailed framework used to calculate lattice thermal conductivity ( $\kappa_{lat}$ ) by considering various phonon scattering mechanisms. These include Umklapp scattering (U-process), where two phonons interact and result in a backward-moving phonon, effectively

reducing thermal conductivity, particularly at higher temperatures. Normal scattering (N-process) involves phonons exchanging energy without changing direction, which does not reduce conductivity but affects energy transfer. Boundary scattering occurs at surfaces or interfaces, especially in nanostructures, reducing the mean free path of phonons. Point defects and dislocations scatter phonons and decrease their mean free path, further lowering thermal conductivity.

The Callaway model expresses lattice thermal conductivity as:

$$\kappa_{lat} = \frac{1}{3} C v_{ph} \frac{1}{\tau_{eff}}$$

$$\kappa_{lat} = \frac{1}{3} C v_{ph} \frac{1}{\tau_{eff}}$$

where  $\tau_{eff}$  is the effective phonon relaxation time. This effective relaxation time is the inverse sum of the individual relaxation times for each scattering mechanism:

$$\frac{1}{\tau_{eff}} = \frac{1}{\tau_U} + \frac{1}{\tau_N} + \frac{1}{\tau_B} + \frac{1}{\tau_P}$$

Here:

$\tau_U$  is the relaxation time due to Umklapp scattering,  $\tau_N$  is the relaxation time due to normal scattering,  $\tau_B$  is the relaxation time due to boundary scattering,  $\tau_P$  is the relaxation time due to dislocations and point defects.

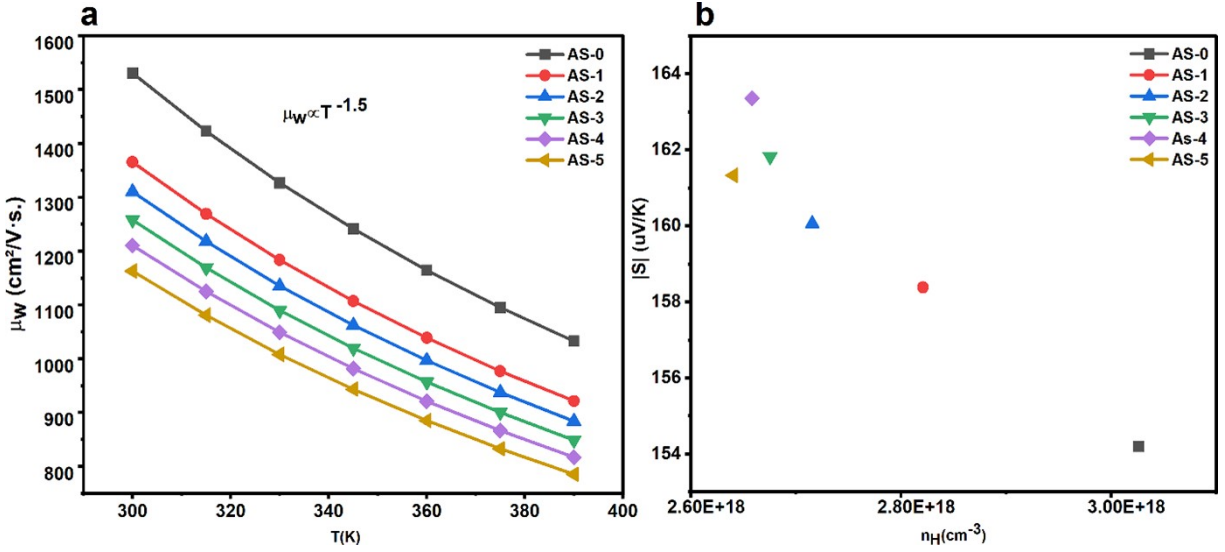


**Fig. S6.** (a) Temperature dependence of weighted mobility ( $\mu_w$ ) exhibiting a  $\mu_w \propto T^{-1.5}$  relationship. (b) Seebeck coefficient ( $|S|$ ) versus carrier concentration ( $n_H$ ), illustrating the influence of  $\text{MoSe}_2$  doping on thermoelectric properties.

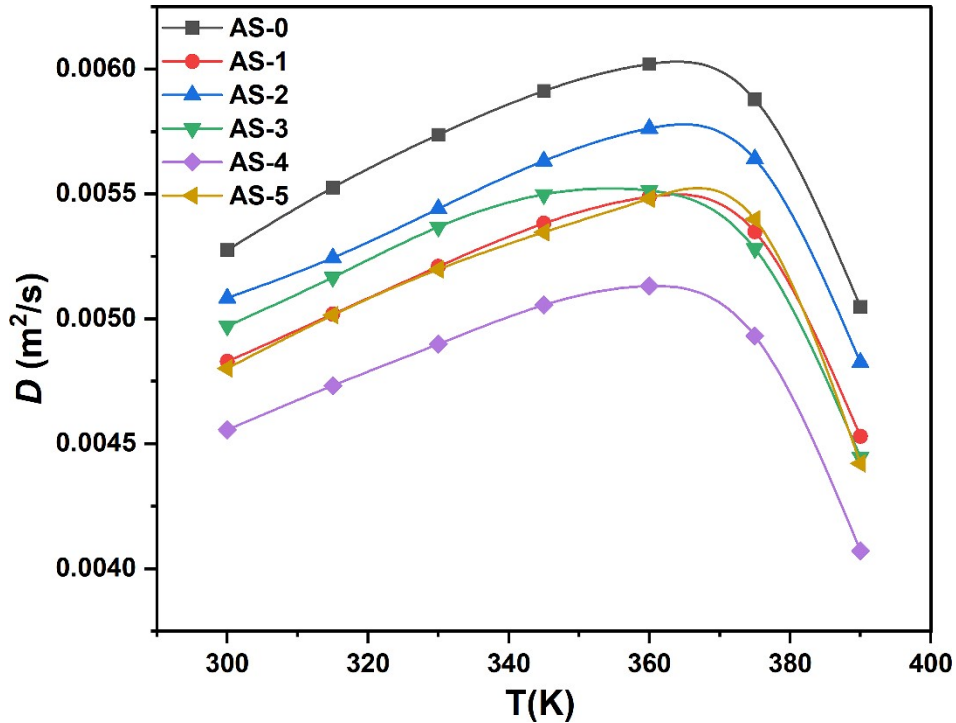


**Fig. S7.** Thermal diffusivity ( $D$ ) of  $\text{Ag}_2\text{Se}/\text{MoSe}_2$  composites (AS-0 to AS-5) as a function of temperature. All samples exhibit an elevation in  $D$  up to 360 K, thereafter followed by a decline. The AS-4 sample has the lowest thermal diffusivity, signifying heightened phonon scattering resulting from interface alterations.

## Device Efficiency Calculation

The efficiency of thermoelectric devices is typically assessed based on electrical power production and the heat absorbed.

$$P = \frac{I^2 R}{2}$$

Where ( $I$ ) is Current in ( $A$ ) and  $R$  is Electrical resistance ( $\Omega$ ).

Alternatively, the power output can be expressed in relation to the Seebeck coefficient.

$$P = \frac{S^2 \Delta T^2 \sigma}{R}$$

$\Delta T$  = Temperature difference across the device

## Heat Transported

The thermal energy conveyed by the thermoelectric device can be computed as

$$Q_h = \kappa \Delta T$$

$Q_h$  is Heat transported ( $W$ ) and  $\Delta T$  is Temperature difference across the device.

## Thermoelectric Device Efficiency

The efficiency ( $\eta$ ) of a thermoelectric device can be defined as the ratio of the useful work output (electrical power) to the total heat input:

$$\eta = \frac{P}{Q_h} = \frac{I^2 R}{2 \kappa \Delta T}$$

Conversely, in an ideal scenario where the device operates in a Carnot cycle with a temperature differential  $\Delta T$  between the hot and cold sides:

$$\eta = \frac{T_{hot} - T_{cold}}{T_{hot}}$$

Where  $T_{hot}$  is Hot side temperature (K) and  $T_{cold}$  Cold side temperature (K).

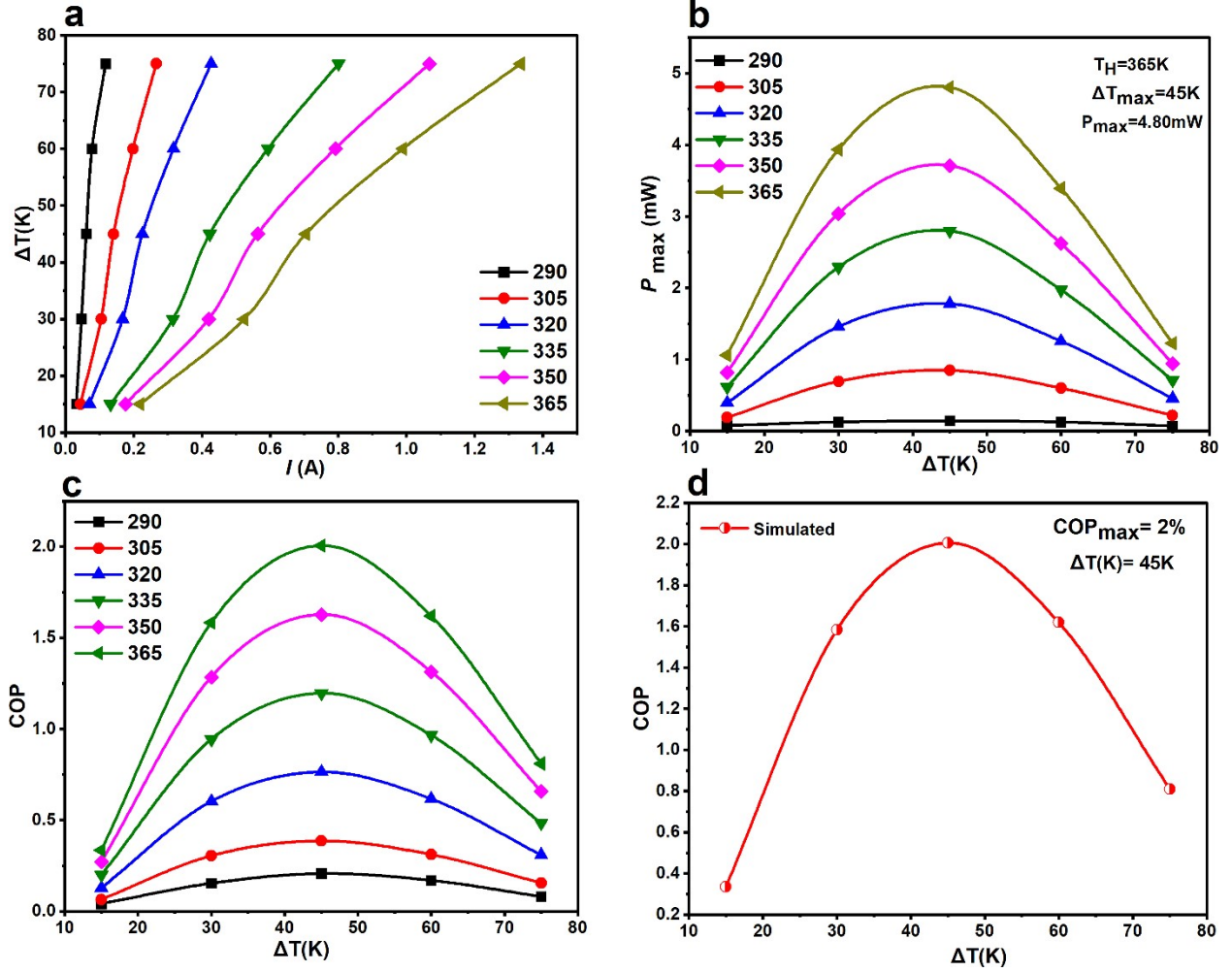


**Fig. S8.** (a) Current-dependent temperature ( $T$ ) at various hot-side temperatures ( $T_h = 290, 305, 320, 330, 335, 350, \text{ and } 365$  K) for the AS-0.4/BST model; (b) Power ( $P$ ) as a function of temperature difference ( $\Delta T$ ) at different hot-side temperatures; (c) Thermoelectric efficiency (COP) as a function of temperature difference ( $\Delta T$ ); (d) Simulated maximum efficiency (COP<sub>max</sub> = 6.27%) at  $\Delta T = 45$  K,